Balanced heterodyne signal extraction in a postmodulated Sagnac interferometer at low frequency

Ke-Xun Sun

TWS Technologies, Inc., 632 Des Moines Place, San Jose, California 95133

Martin M. Fejer, Eric K. Gustafson, and Robert L. Byer

Edward L. Ginzton Laboratory, Stanford University, Stanford, California 94305-4085

Received May 15, 1997

We describe a balanced-heterodyne postmodulated Sagnac interferometer signal extraction method that is suitable for gravitational wave detection. The method is simple to implement by placement of a polarization-selective modulator after the beam splitter in the dark port of the interferometer. The postmodulated Sagnac interferometer retains its common path advantage and exhibits insensitivity to laser frequency noise below, at, and above the heterodyne frequency. Balanced detection reduces sensitivity to laser amplitude noise. In this scheme mirror displacement signals were rf demodulated and observed from 0.2 to 10 kHz. © 1997 Optical Society of America

PACS numbers: 04.80.Nn, 07.60.Ly, 42.25.Hz, 42.62.-b

In advanced gravitational wave laser interferometers[1] incident laser powers of 100 W with circulating powers within the interferometer of as much as 1 MW are expected. There is a need for a signal extraction scheme that is simple to implement for detecting signals in the 10-Hz to 10-kHz frequency region and that avoids thermally induced beam distortions resulting from modulators placed within[2,3] or before[4] the interferometer. We propose and demonstrate a signal extraction method in which the modulator is placed after the beam splitter in the dark port of a Sagnac interferometer.[5] This scheme both preserves the common path advantage of the Sagnac interferometer and permits balanced detection.

Heterodyne detection is necessary in low-frequency interferometric signal detection such as that involved in gravitational wave and rotation sensing.[6] Early Michelson gravitational wave detectors and traditional Sagnac interferometers used in-arm or in-loop frequency modulators.[2,3,6] Recent research has used a modulator before the interferometer,[4] a post-beam-splitter modulator at the dark port,[7] or external modulation with a Mach–Zehnder configuration[8,9] at the output of the interferometer to generate a local oscillator. The schemes of Refs. 2–4 and 6 are relatively simple to implement but require that modulators handle high optical power. The schemes of Refs. 7–9 operate at lower powers transmitted through the optical modulators but add complexity by requiring additional optical elements and their control.

In this Letter we report an extension to low frequencies of the polarization-based signal extraction scheme of Ref. 10 by placing a phase modulator after the interferometer beam splitter in the dark port to generate a heterodyne local oscillator. Our postmodulation signal extraction scheme uses the polarization-dependent interference in a Sagnac interferometer with a polarization-dependent beam splitter to produce, in response to the relative motion of the interferometer mirrors,[2] relative phase shift and an amplitude difference between the orthogonally polarized signal and local-oscillator field output from the interferometer. A polarization-dependent phase modulator preferentially modulates one of the polarizations to generate sidebands at the heterodyne frequency. Combined with the carrier transmission asymmetry, this polarization-selective postmodulation approach permits balanced heterodyne detection while preserving a common path in the interferometer for the signal and the local oscillator. The balanced detection in this postmodulation method reduces sensitivity to laser amplitude noise, and the common path for the signal and the local oscillator beams preserves the common path advantages of the Sagnac interferometer as described in Ref. 5.

Figure 1 is a schematic of the experimental setup, which is similar to that described in Ref. 10. The essential components are the Sagnac interferometer with a polarization-dependent beam splitter and a polarization-sensitive phase modulator placed in the dark port after the beam splitter of the interferometer. The displacement signal is provided by piezoelectrically driving arm mirrors 180° out of phase. The time-dependent differential displacements of the mirrors produce dynamic phase shifts ϕ_{ccw} and ϕ_{cw} for counterclockwise and clockwise waves, respectively. The interferometer output field for each polarization is given by

$$E_{\mathrm{out}}^{(m)} = [t^{(m)^2} \exp(i\phi_{\mathrm{ccw}}) - r^{(m)^2} \exp(i\phi_{\mathrm{cw}})] E_{\mathrm{in}}^{(m)}, \tag{1}$$

where $m = s$ or $m = p$ for the s or p polarization $t^{(m)}$ and $r^{(m)}$ are amplitude transmittivity and reflectivity of the beam splitter, and $E_{\mathrm{in}}^{(m)}$ and $E_{\mathrm{out}}^{(m)}$ are input and output fields, respectively. For the normal Sagnac interferometer with a signal in the s polarization, we choose $R^{(s)} = r^{(s)^2} = T^{(s)} = t^{(s)^2} = 0.5$,

0146-9592/97/191485-03$10.00/0

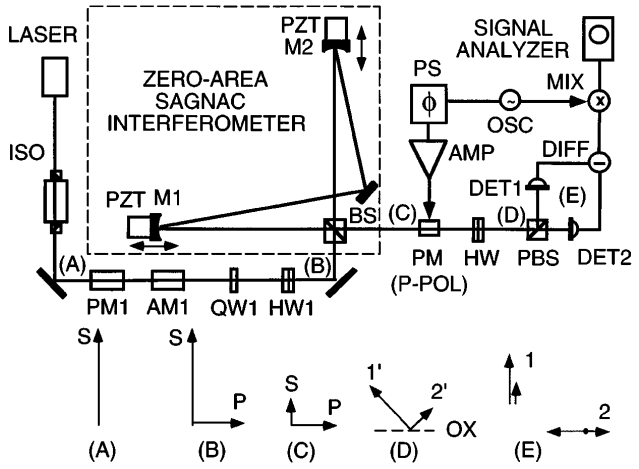

Fig. 1. Experimental setup and the polarization states at several positions in the system: LASER, 300-mW Nd:YAG laser; ISO, Faraday isolator. PM, PM1, electro-optic phase modulators; AM1, electro-optic amplitude modulators; HW, HW1, half-wave plates; QW1, quarter-wave plate; M1, M2, arm mirrors; BS, beam splitter; PBS, polarizing beam splitter; OX, transmission polarization axis of the polarizing beam splitter; DET1, DET2, detectors for polarization projections 1 and 2, respectively; DIFF, difference port of a rf hybrid junction; MIX: double-balanced rf mixer as a demodulator; OSC, rf oscillator at 96 MHz; PS, rf phase shifter; AMP, rf amplifier. Polarization states at locations (A)–(E) are drawn below the experimental setup.

and the output field is given by $E_{\mathrm{out}}{}^{(s)} = i\,\exp[i(\phi_{\mathrm{ccw}} + \phi_{\mathrm{cw}})/2]\sin(\Delta\phi/2)E_{\mathrm{in}}{}^{(s)}$, where the differential phase is defined as $\Delta\phi = (\phi_{\mathrm{ccw}} - \phi_{\mathrm{cw}})$.[5] For the local oscillator in the p polarization, $R^{(p)} = 0$ and $T^{(p)} = 1$ $E_{\mathrm{out}}{}^{(p)} = \exp(i\phi_{\mathrm{ccw}})E_{\mathrm{in}}{}^{(p)}$. The amplitudes and phases of $E_{\mathrm{out}}{}^{(s)}$ and $E_{\mathrm{out}}{}^{(p)}$ differ because of the polarization-dependent interference, even though the signal and the local oscillator waves experience the same optical path inside the interferometer.

The phase modulator placed in the dark port of the interferometer is an electro-optic crystal oriented to modulate preferentially the p-polarized carrier to generate sidebands that serve as the heterodyne local oscillator. The two polarization components are superimposed in phase and out of phase at two ports of a properly oriented polarizing beam splitter. The heterodyne signal is contained in the difference current

$$\begin{aligned} I_1 - I_2 &= \eta_1|[E_{\mathrm{out}}{}^{(s)} + E_{\mathrm{out}}{}^{(p)}]/\sqrt{2}|^2 - \eta_2 \\ &\quad \times |[E_{\mathrm{out}}{}^{(s)} - E_{\mathrm{out}}{}^{(p)}]/\sqrt{2}|^2 \\ &= 2\eta\ \mathrm{Re}[E_{\mathrm{out}}{}^{(p)}E_{\mathrm{out}}{}^{(s)*}], \end{aligned} \tag{2}$$

where the system efficiencies for channels 1 and 2, η_1 and η_2, respectively, are set equal to η. A heterodyne beat signal can be produced only by preferential phase modulation of one of the polarization components. We chose to modulate the polarization containing the local oscillator rather than that containing the signal to minimize disturbance to the signal.

To test this signal detection scheme we used a 300-mW diode-pumped Nd:YAG laser to illuminate the tabletop Sagnac interferometer. The purpose of the experiment was to explore the postmodulation scheme and not to achieve the highest degree of phase sensitivity. A half-wave plate and a quarter-wave plate produced a small p-polarized component at the input to the Sagnac interferometer for use as the local oscillator. The beam splitter was 50% transmissive for the s polarization and 99% transmissive for the p polarization. Therefore the s-polarized waves produced a dark fringe at the output, except for a small leakage of 0.23 mW, giving a contrast ratio $C = 0.9985$. The power transmission of the Sagnac interferometer for the p-polarized carrier was $(0.99-0.01)^2 \approx 0.96$.[10] Arm mirrors M1 and M2, located 550 and 560 mm away from the beam splitter, respectively, and 1119 mm apart from each other, were mounted upon piezoelectric translators (PZT's) that permitted several micrometers of motion. A $LiNbO_3$ electro-optic phase modulator was oriented to modulate the p-polarized carrier preferentially to provide the local oscillator. The phase modulator was operated at a 96-MHz heterodyne frequency with a modulation depth of 1.19 rad and with phase adjustable by a phase shifter. For the convenience of placing detectors in the tabletop plane, a half-wave plate with its optical axis oriented 22.5° from the vertical (s-polarization) plane was used after the phase modulator to rotate the s polarization by 45° clockwise and the P polarization by 135° counterclockwise. A polarizing beam splitter projected the two polarizations onto two detectors, whose photocurrents were fed to a rf hybrid junction. The difference signal was demodulated at 96 MHz by a double-balanced mixer and then measured with a signal analyzer.

Figure 2(a) shows the spectral density of differential phase $\Delta\phi$ induced by the differential motion of the mirrors, which were driven by PZT's with 1-kHz triangle waves, which were 180° out of phase. The triangle waveform was chosen such that Fourier sidebands would be generated across the 1–10-kHz frequency region of interest to gravitational wave detection. The calibration peak at 1 kHz was obtained by independent measurement of the $\Delta x = 18$ nm mirror displacement, which corresponds to a phase modulation of $4\pi\Delta x/\lambda = 0.22$ rad. The differential phase is reduced by the Sagnac interferometer response function[5] at 1 kHz to $\Delta\phi = 9.97$ μrad. The differential optical phase was observed with a signal-to-noise ratio of 20 dB above the noise floor, which at 1 kHz had comparable contributions from acoustic and electronic noise as expected from a tabletop experiment. Above 3 kHz the noise spectrum was dominated by electronic noise, which is flat with frequency. The signal peaks at frequencies of 3, 5, 7, and 9 kHz were produced mainly by Fourier harmonics of the triangle waveform. Peaks were not observed at 4, 6, and 8 kHz, where the Bessel sidebands were below the noise floor. Peaks at greater than 5 kHz increased in amplitude because of mechanical resonances in the PZT's.

Figure 2(b) compares balanced detection with the unbalanced detection that we obtained by blocking one of the detectors. The laser amplitude noise in the range 0–3 kHz is increased in Fig. 2(b) from that in Fig. 2(a). The measurement demonstrates common mode rejection of the laser amplitude noise of 40 dB in power near 200 Hz. The peaks observed at 2, 4, 6, and 8 kHz in Fig. 2(b) were due to amplitude

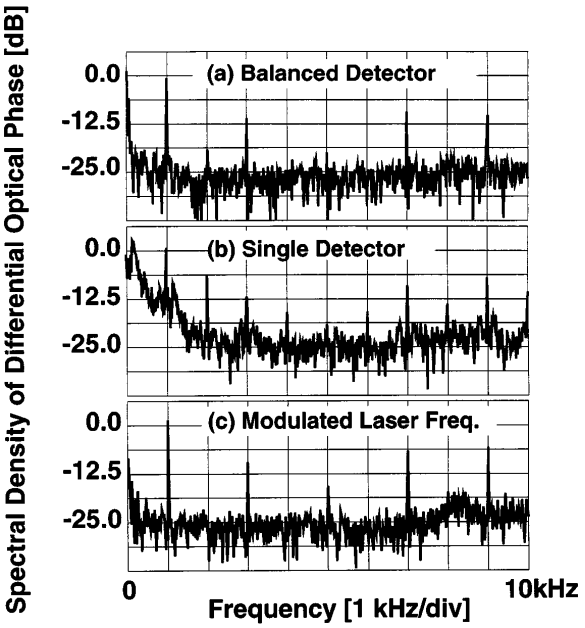

Fig. 2. Spectral density of the difference photocurrent converted to differential phase. The vertical scale is 12.5 dB/division for electrical power and 6.25 dB/division for differential optical phase. The calibration peak at 1 kHz is for a measured 18-nm mirror displacement corresponding to a 9.97-μrad differential optical phase signal. The IF resolution bandwidth is 18.7 Hz. (a) Balanced detection, demonstrating the low-frequency signal extraction and common mode rejection of laser- and mirror-tilt-induced amplitude noise. (b) Spectrum taken when one of the detectors was blocked to disable balanced detection. As much as 20 dB of excess amplitude noise is evident from 0 to 3 kHz and at peaks at 2, 4, 6, and 8 kHz. (c) Differential phase measurement with frequency and phase modulation applied to the input laser (see text for details). The signal extraction and the noise floor, and thus the phase sensitivity, were not affected by laser frequency modulation.

noise resulting from inadvertent PZT-induced mirror tilts, which caused an asymmetrical perturbation to the pointing of the counterclockwise and clockwise waves that varied the degree of interference on the beam splitter. The modulated dark fringe resulted in amplitude modulation in the detected power. In Fig. 2(a), for which balanced detection was used, these amplitude noise peaks were largely suppressed, as expected.

Figure 2(c) shows a differential phase measurement taken to demonstrate the robustness of the signal extraction scheme against laser frequency and phase noise. The laser frequency and phase modulation consisted of a fast modulation obtained by application of a 20-Hz triangle-wave voltage to a PZT bonded to the Nd:YAG laser crystal to produce a frequency excursion of 105 MHz, a 2.5-GHz peak-to-peak frequency shift at a rate of 0.1 Hz obtained by scanning of the laser-crystal temperature, and a phase modulation centered at 96 MHz with a modulation depth of 0.1 mrad introduced onto the laser beam through electro-optic phase modulator PM1. The measured differential phase signals were not affected, and there was no significant change in the noise floor in the presence of these multiple laser frequency and phase modulations.

In conclusion, we have proposed and experimentally demonstrated a balanced heterodyne signal extraction scheme at low frequencies in a postmodulated Sagnac interferometer. Using this method, we performed interferometric differential phase measurements at frequencies from 10 Hz to 10 kHz. We demonstrated the robustness of the detection method against laser amplitude and frequency noise and mirror-tilt-induced amplitude noise. The scheme can be extended to other interferometer topologies with polarization-selective beam splitters, such as the Michelson–Fabry–Perot interferometer configuration including the power and dual-recycled version proposed for laser gravitational wave detectors, although a more-complex geometry may be required.[11] The shot-noise-limited phase sensitivity of this signal extraction scheme is similar to that of the Michelson–Mach–Zehnder interferometer previously described for gravitational wave detectors[3] but offers the advantages of simpler implementation and the use of optical phase modulators at low incident optical power levels.

This research was supported by the National Science Foundation (NSF PHY 9212157 and 9630172). We thank D. Shoemaker (Massachusetts Institute of Technology), R. Abbott (California Institute of Technology), and C. Harb (Australian National University) for useful discussions.

References

1. A. Abramovici, W. E. Althouse, R. W. P. Drever, Y. Gursel, S. Kawamura, F. J. Raab, D. Shoemaker, L. Sievers, R. E. Spero, K. S. Thorne, R. E. Vogt, R. Wiess, S. E. Whitcomb, and M. E. Zucker, Science **256,** 325 (1992).
2. R. Weiss, MIT Res. Lab. Electron. Q. Rep. **105,** 54 (1972).
3. D. Shoemaker, P. Fritschel, J. Giaime, N. Christensen, and R. Weiss, Appl. Opt. **30,** 3133 (1991).
4. M. W. Regehr, F. J. Raab, and S. E. Whitcomb, Opt. Lett. **20,** 1507 (1995).
5. K.-X. Sun, M. M. Fejer, E. K. Gustafson, and R. L. Byer, Phys. Rev. Lett. **76,** 3053 (1996).
6. S. Ezekiel and H. J. Arditty, eds., *Fiber-Optic Rotation Sensors* (Springer-Verlag, Berlin, 1982).
7. C. N. Man, D. Shoemaker, M. P. Tu, and D. Dewey, Phys. Lett. **148,** 8 (1990).
8. J. Giaime, "Studies of laser interferometer design and a vibration isolation system for interferometric gravitational wave detectors," Ph.D dissertation (Massachusetts Institute of Technology, Cambridge, Mass., 1995).
9. M. B. Gary, A. J. Stevenson, C. C. Harb, H.-A. Bachor, and D. E. McClelland, Appl. Opt. **35,** 1623 (1996).
10. K.-X. Sun, E. K. Gustafson, M. M. Fejer, and R. L. Byer, Opt. Lett. **22,** 1359 (1997).
11. K. X. Sun, Bull. Am. Phys. Soc. **42,** 1106 (1997).